Sharkskin-Mimetic Desalination Membranes with Ultralow Biofouling

Wansuk Choi,[a,‡] Changhoon Lee,[a,‡] Young June Won,[b,‡] Dahye Lee,[b] Gi Wook Lee,[a] Min Gyu Shin,[a] Byoungjin Chun,[a] Taek-Seung Kim,[c] Hee-Deung Park,[c] Hyun Wook Jung,[a,]* Jong Suk Lee,[b,]* Jung-Hyun Lee[a,]*

[a]Department of Chemical and Biological Engineering, Korea University, 145 Anam-ro, Seongbuk-gu, Seoul 02841, Republic of Korea, *E-mail: hwjung@grtrkr.korea.ac.kr; leejhyyy@korea.ac.kr

[b]Department of Chemical and Biological Engineering, Sogang University, 35 Baekbeom-ro, Mapo-gu, Seoul 04107, Republic of Korea, *E-mail: jongslee@sogang.ac.kr

[c]School of Civil, Environmental and Architectural Engineering, Korea University, 145 Anam-ro, Seongbuk-gu, Seoul 02841, Republic of Korea.

Table S1. The quality of natural seawater.

	pH	Conductivity (mS)	Turbidity (NTU)	TDS (g/L)	TOC (mg/L)
Raw water	6.8 ± 0.2	37.1 ± 0.4	0.53 ± 0.3	43.3 ± 0.4	19.6 ± 0.6
Pretreated water	6.7 ± 0.1	36.9 ± 0.3	0.36 ± 0.4	42.7 ± 0.3	15.2 ± 0.5

Collected natural seawater was pretreated with a microfiltration filter (0.45 μm pore size) to remove large foulants. Raw and pretreated seawater was characterized using various analyzing methods. A pH meter (Orion Star A221, Thermo Fisher Scientific, Waltham, MA) was used to determine pH of water, while an Ultrameter II (Myron L Company, Carlsbad, CA) was employed to analyze the conductivity and total dissolved solids (TDS) of seawater. Turbidity was measured using a turbidity meter (Hach 2100P, Hach Company, Loveland, CO). A total organic carbon (TOC) analyzer (Sievers 900, GE Analytical Instruments, Boulder, CO) was used to measure the organic concentration of water.

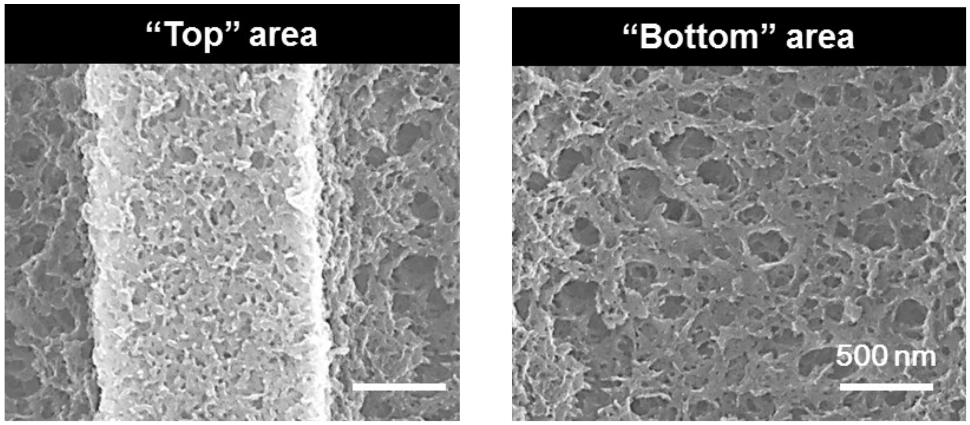

Position	Surface Pore Size (nm)	Surface Porosity (%)
Top	25 ± 8	29 ± 2
Bottom	99 ± 12	54 ± 3

Fig. S1. The magnified SEM images of the pattern of the top and bottom base surfaces. The average surface pore size and surface porosity were quantified from the black-and-white images converted from the original SEM images using the ImageJ program.

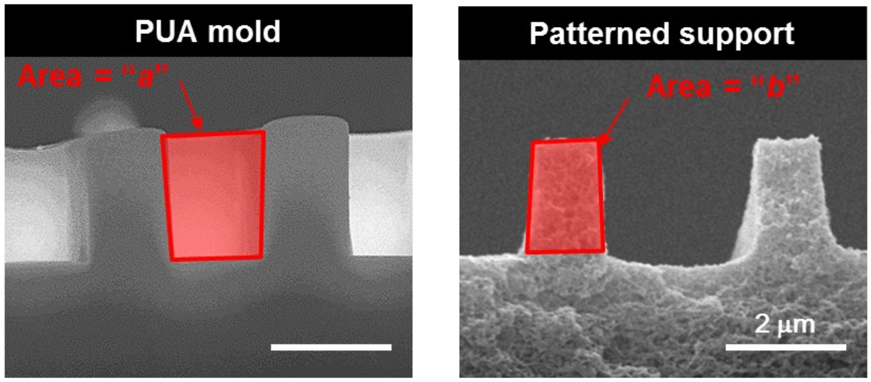

$$\text{Fidelity} = \frac{\text{Pattern cross-sectional area of a membrane}}{\text{Mold pattern cross-sectional area for replication}} = \frac{b}{a}$$

Pattern	Fidelity (b/a)
Line	76.0 ± 4.9%
D. line	74.9 ± 4.3%
Sharklet RC	75.5 ± 4.9%
Sharklet AF	74.4 ± 2.6%

Fig. S2. A method to calculate the pattern fidelity and calculated fidelity data for the patterned support membranes. The pattern fidelity was calculated from the ratio of the pattern cross-sectional area of the patterned membrane (denoted as "*b*") to the mold pattern cross-sectional area for replication (denoted as "*a*").[1,2] Each area was calculated using the ImageJ software on the corresponding SEM cross-sectional images of the membrane and mold.

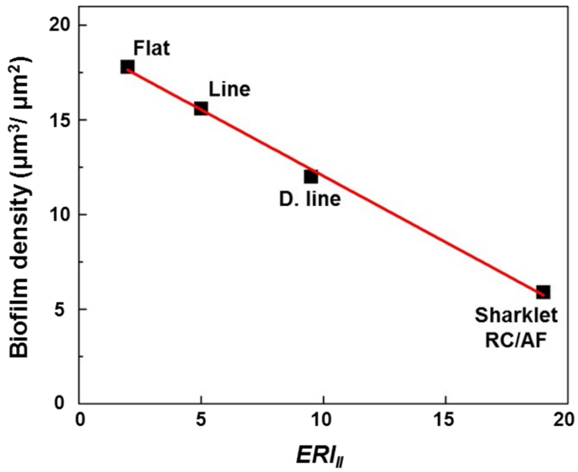

Membrane	r	n	φ	ERI_{II}
Flat	1	1	0	1
Line	2.5	1	0.50	5
D. line	2.44	2	0.55	9
Sharklet RC	2.5	4	0.53	19
Sharklet AF	2.4	4	0.55	19

Fig. S3. A plot of biofilm density versus ERI_{II} values of the patterns (left). The ERI_{II} values were calculated from the geometry parameters (r: roughness, n: the number of the distinct pattern features denoting the pattern complexity and φ: the area fraction of the protruded pattern region) of the corresponding patterns (right).

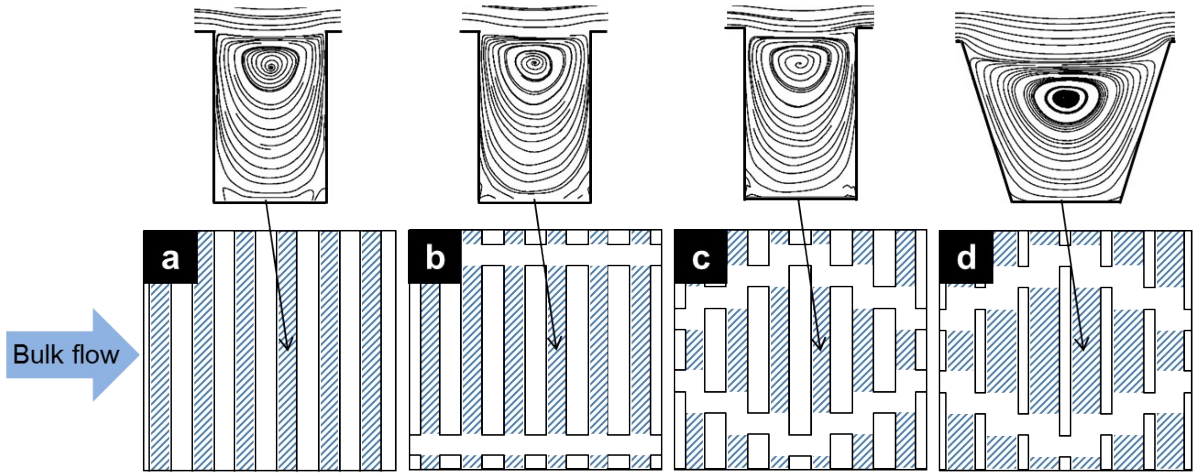

Area percentage of vortex forming region (%)			
Line	D. line	Sharklet RC	Sharklet AF
50	44.4	29.6	44.4

Fig. S4. The cross-sectional shape, distribution and area percentage of the vortices formed for the (a) line, (b) D. line, (c) Sharklet RC and (d) Sharklet AF patterns aligned perpendicular to the bulk flow direction. The blue colored area indicates the vortex forming region.

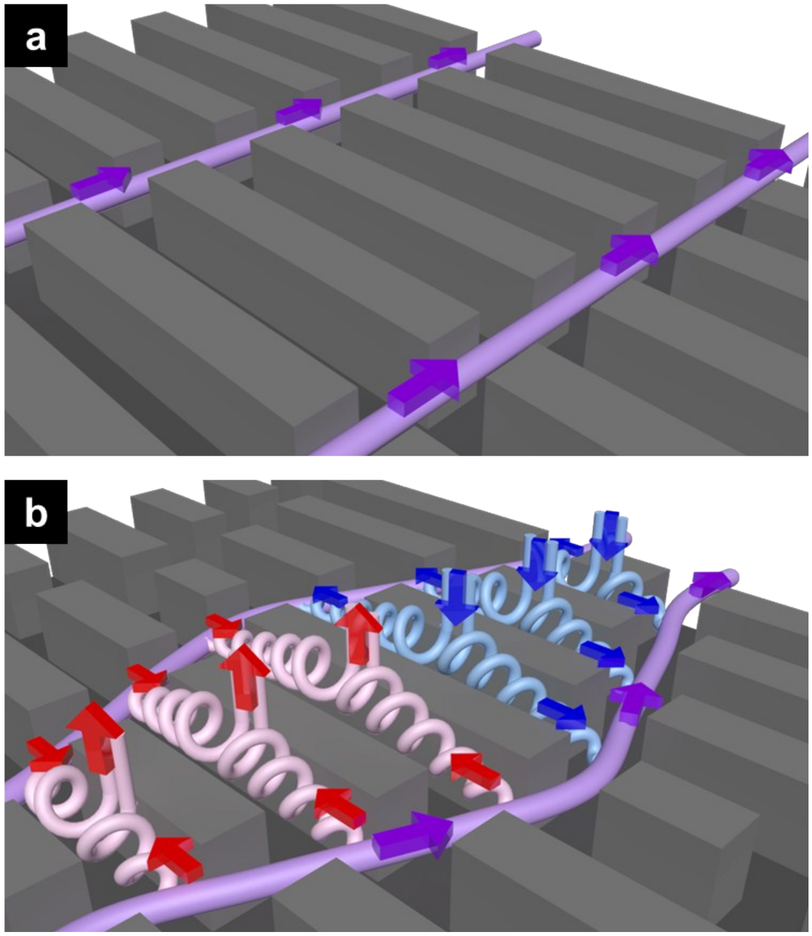

Fig. S5. Schematic three-dimensional diagram of the local flow for the (a) D. line and (b) Sharklet patterns. Purple line: the primary flow, red line: the secondary flow leaving the pattern surface, blue line: the secondary flow entering the pattern surface.

References

1 A. Bessonov, J. W. Seo, J. G. Kim, E. S. Hwang, J. W. Lee, J. W. Cho, D. J. Kim, S. Lee, *Microelectron. Eng.,* 2011, **88**, 2913.

2 Y.-J. Won, D.-C. Choi, J. H. Jang, J.-W. Lee, H. R. Chae, I. Kim, K. H. Ahn, C.-H. Lee, I.-C. Kim, *J. Membr. Sci.,* 2014, **462**, 1.